Nanostructures

DOI: 10.1002/anie.201105789

Reinforced Multifunctionalized Nanofibrous Scaffolds Using Mussel Adhesive Proteins**

*Bum Jin Kim, Yoo Seong Choi, and Hyung Joon Cha**

Nanofiber technology has been largely recognized because of its ability to fabricate multiple nanosized fibers that are structurally similar to collagen fibrils of the natural extracellular matrix (ECM).[1] The large surface area of nanofibers is a major advantage of nanofibrous scaffolds because these are the sites at which cell–substrate interactions occur. Rendering the nanofiber surface to be biofunctional is critical for its successful application in tissue engineering.[2] Synthetic and natural biomaterials have been widely used for the fabrication of nanofibrous scaffolds for tissue engineering applications.[3] Blending synthetic and natural biomaterials has been used to combine the excellent biological activities of natural biomaterials with the high processability and desired mechanical strengths of synthetic polymers; however, this approach has had limited success for several pairs of synthetic and natural biomaterials.[2a]

Several bioactive molecules, such as ECM proteins, ECM carbohydrates, ECM-derived peptides, and growth factors, have been introduced onto the surface of nanofibers to design biofunctional and biomimetic tissue engineering scaffolds.[4] Generally, typical conjugation chemistry and physical adsorption procedures have been used to immobilize biomolecules after the completion of the surface activation steps, including plasma and wet-chemical treatments or surface graft polymerization.[5] However, these strategies are limited in availability because of the multiple, complicated procedures that are required to complete them. Thus, development of a simple and effective surface functionalization strategy for nanofibers would be a promising tool for successful tissue engineering applications.

[*] Prof. H. J. Cha
Department of Chemical Engineering, Ocean Science and Technology Institute, Pohang University of Science and Technology
Pohang 790-784 (Korea)
E-mail: hjcha@postech.ac.kr
Homepage: http://magic.postech.ac.kr

B. J. Kim
School of Interdisciplinary Bioscience and Bioengineering Pohang University of Science and Technology, Pohang 790-784 (Korea)

Prof. Y. S. Choi
Department of Chemical Engineering
Chungnam National University, Daejon 305-764 (Korea)

[**] Financial support was provided by the Marine Biomaterials Research Center grant from Marine Biotechnology program funded by the Ministry of Land, Transport and Maritime Affairs (Korea), the National Research Laboratory program (ROA-2007-000-20066-0) funded by the Ministry of Education, Science and Technology (Korea), and the Rising Star program funded by POSTECH.

Supporting information for this article is available on the WWW under http://dx.doi.org/10.1002/anie.201105789.

In the present work, we propose to use mussel adhesive protein (MAP) as a natural biomaterial that serves as a blending partner for the preparation of sticky nanofibrous scaffolds. Using MAPs as a blending partner provides a facile, efficient, and multifunctionalizing platform for generating novel nanofibrous scaffolds. In fact, nanofibrous scaffolds based on MAPs having mechanical reinforcement were fabricated by a simple e lectrospinning process to develop a "general coating platform" for diverse bioactive molecules (Figure 1).

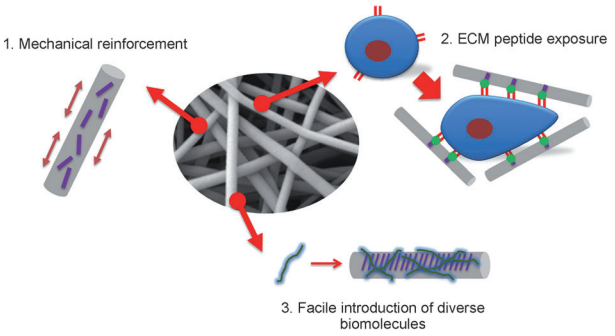

Figure 1. Schematic representation of various functionalized MAP-based nanofibrous scaffolds.

Marine mussel adhesion is known to be mediated by MAPs, which are secreted by mussel feet and have great potential as biologically and environmentally friendly biomaterials because of their biocompatibility and biodegradability.[6] In addition, MAPs have strong adhesion ability, even on wet surfaces, as a result of unique amino acid arrangements and composition.[6d] However, research using the natural amino acid composition of MAPs has been limited because of difficulties in obtaining sufficient quantities of MAPs for applications. Recently, genetically redesigned fusion MAP, fp-151, was successfully and massively produced using a bacterial expression system, and this fusion protein showed significant adhesion ability.[7a] In addition, using the superior cell adhesion properties and fusion technology of the bioactive ECM peptides, we discovered the great potential of MAPs as biofunctional biomaterials for tissue engineering applications.[7] Here, for the first time, we report on the multifunctional roles of MAPs as components of nanofibrous scaffolds.

Prior to this study, the electrospinning of MAPs had not been reported. Therefore, it was necessary to establish appropriate MAP electospinning conditions. Because fp-151 is a basic protein with a calculated isoelectric point (pI) value of 9.91, a cosolvent of 1,1,1,3,3,3-hexafluoroisopropanol

(HFIP) and acetic acid was used for electrospinning, and a nanofiber was successfully fabricated using a 12 wt% concentration of a fp-151 solution (see Figure S1 in the Supporting Information). Although the fabrication of nanofibers using pure MAP was achieved, these nanofibers were not adequate for use because of mechanical weaknesses and easy dissolution in aqueous solutions. Composite nanofibers were fabricated by blending MAP fp-151 with mechanically sound, synthetic polymers to impose mechanical endurance, the desired surface structure, and biological activity to the nanofibers. The synthetic polymers were used as fibrous backbones, and MAP was used as a cell supporter and linking material with other biological compounds to provide adequate cell–fiber interactions.

Our results demonstrate that fp-151 was successfully electrospun into nanofibers with several biodegradable, synthetic polymer-blending partners, many of which are commonly used for tissue engineering applications, including polycaprolactone (PCL), polydioxanone (PDO), poly(L-lactide) (PLLA), poly(DL-lactide-co-glycolide) (PLGA), polyethylene oxide (PEO), and polyvinyl alcohol (PVA; Figure 2). Because PCL, PDO, PLLA, and PLGA are

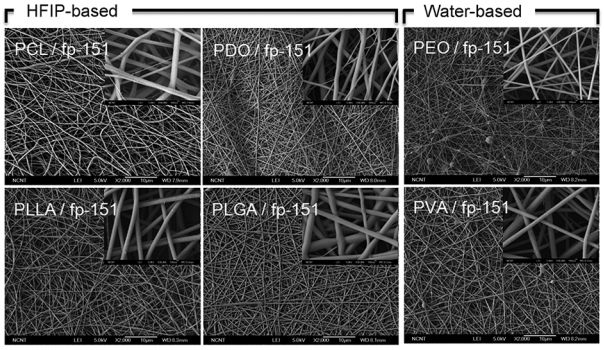

Figure 2. SEM images of electrospun nanofibers made from a MAP-based composite with various synthetic polymer partners. The nanofibers are either HFIP- or water-based depending on the solvent used. Ratios (wt/wt) used: PCL/fp-151 = 70:30; PDO/fp-151 = 70:30; PLLA/fp-151 = 90:10; PLGA/fp-151 = 90:10; PEO/fp-151 = 70:30; PVA/fp-151 = 70:30. The scale bar is 10 μm.

typically electrospun with HFIP, we determined that a 12 wt% concentration of fp-151 as a cosolvent with HFIP and acetic acid was appropriate for blending. Moreover, because fp-151 dissolves well in water, PEO and PVA, which can be electrospun in a water-based solvent, were also used as partners with MAPs. These results indicate that this blending strategy worked well for the fabrication of MAP-based nanofibers and suggest that MAPs can be used with a variety of polymer partners to fabricate composite nanofibers.

Next, PCL was selected as a model blending partner for additional analysis of the fabricated composite nanofibers; the hypothesis was that the relatively low stiffness and high flexibility of PCL would synergistically compensate for the less desirable properties of pure MAP nanofibers. Moreover, PCL had been previously used to develop composite nanofibers with gelatin and collagen for tissue engineering.[8] Nanofibers were finely electrospun using various PCL:fp-151 ratios (100:0, 90:10, 70:30, and 50:50) of the blending solutions 6 wt% PCL and 12 wt% fp-151, and they were not dispersed in an aqueous solution without any cross-linking (see Figure S1 in the Supporting Information). This electrospinning resulted in nanofibers with diameters estimated to be from 170 nm to 230 nm and porosity ranging from 77% to 82% (see Table S1 in the Supporting Information). The mechanical properties of the PCL/fp-151 nanofibers were characterized by measuring tensile properties. After obtaining stress-strain curves (see Figure S2a in the Supporting Information), tensile strength, elongation, and Young's modulus were determined and compared (Table 1). While PCL

Table 1: Mechanical properties of PCL/fp-151 nanofibers.[a]

Nanofiber	PCL/MAP	Strength [MPa]	Elongation [%]	Modulus [MPa]
PCL	100:0	4.1 ± 0.3	170.9 ± 22.3	13.2 ± 4.0
PCL/fp-151	90:10	18.1 ± 2.8	107.0 ± 34.7	44.3 ± 9.1
PCL/fp-151	70:30	10.7 ± 2.8	75.8 ± 10.8	29.9 ± 3.5
PCL/fp-151	50:50	6.8 ± 2.9	54.7 ± 23.4	28.2 ± 12.8

[a] The values for each parameter were obtained from the stress-strain curves of each nanofiber. See the Supporting Information for experimental details.

nanofibers showed soft and flexible properties as expected, the PCL/fp-151 nanofibers became stiff and brittle as the fp-151 content increased. Interestingly, the PCL/fp-151 = 90:10 nanofiber showed the highest tensile strength of approximately 18 MPa, which was fourfold higher than that of a PCL nanofiber; and PCL/fp-151 = 70:30 still showed a high tensile strength of approximately 10 MPa. Although the elongation was gradually decreased as the fp-151 content increased, PCL/fp-151 = 90:10 and PCL/fp-151 = 70:30 showed relatively high elongations of 107% and 75%, respectively. There have been several controversial reports about the incorporation of natural polymers, such as collagen and gelatin, and how these polymers can influence the mechanical properties of composite nanofibers.[11] Through the comparative experiment using gelatin as a control natural polymer, we also found similar reinforcing tendency that the tensile strength and Young's modulus were increased, and elongation was decreased by addition of gelatin (more than 30%) into PCL/gelatin nanofibers. However, their tensile strengths were about half of the values measured for the PCL/fp-151 nanofibers (see Figure S2b in the Supporting Information). Our experimental results might be explained by X-ray diffraction (XRD) analysis (see Figure S3 in the Supporting Information). The XRD analysis showed that the PCL/fp-151 = 90:10 and PCL/fp-151 = 70:30 nanofibers had more intense and steeper peaks at $2\theta = 21°$ and 23° compared to those of the PCL nanofiber; and the peak of PCL/fp-151 = 50:50 decreased. This indicates that the PCL/fp-151 = 90:10) and PCL/fp-151 = 70:30 nanofibers have higher crystallinity, which may cause enhanced tensile strength. Our results on the mechanical properties of PCL/fp-151 nanofibers clearly demonstrate that the incorporation of fp-151 through the blending strategy described herein strengthened the rigidity of the composite nanofibers in the case of PCL. The versatile use of MAPs with various polymer partners can be applied to

modify mechanical properties of polymer/MAP composite nanofibers.

Surface properties were also investigated to determine whether fp-151 was exposed on the surface during the incorporation of fp-151 into the PCL/fp-151 nanofibers. First, the contact angle was measured to estimate the surface hydrophilicity of the electrospun nanofibers. The contact angle of the nanofibers decreased as the fp-151 content increased, whereas the contact angle remained consistently high for PCL nanofibers (see Figure S4 in the Supporting Information). This difference might be due to the exposure of the hydrophilic residues of fp-151. Second, Fourier-transform infrared (FT-IR) analysis was performed to characterize the surface functional groups. FT-IR spectra indicated that the PCL and PCL/fp-151 nanofibers both had similar infrared spectra with respect to the PCL-related stretching modes,[9] but common bands of proteins were observed only for the PCL/fp-151 nanofibers; the bands were at approximately $\nu = 1650\ cm^{-1}$ (amide I) and $\nu = 1540\ cm^{-1}$ (amide II; see Figure S5 in the Supporting Information). These values corresponded to the stretching vibrations of C=O bonds and the coupling of the bending of N–H bond and stretching of C–N bonds, respectively. Thus, the appearance of amide groups in the FT-IR spectra indicated that the peptide bonds of fp-151 were detected. Third, X-ray photoelectron spectroscopy (XPS) analysis was performed to identify atomic components on the surface of the PCL/fp-151 nanofibers. The number of the nitrogen components, which were not detected on the PCL nanofibers, gradually increased as the fp-151 content of the PCL/fp-151 nanofibers increased (see Table S2 in the Supporting Information). These experiments confirmed that fp-151 was successfully exposed on the surface of the composite nanofibers.

Next, we investigated cell behavior on PCL/MAP nanofibers. For this in vitro cell culture study, PCL/fp-151 nanofibers with a constant mixing ratio of 70:30 were selected because this ratio demonstrates a good balance of mechanical properties (Table 1) and had the best ability for cell attachment compared to other PCL/fp-151 nanofibers having different ratios (data not shown). In addition to the PCL and PCL/fp-151 = 70:30, PCL/fp-151-RGD = 70:30 was also used as a matrix in the cell culture study. The MAP fp-151-RGD contains a cell recognition ECM peptide, GRGDSP, at the C-terminus of fp-151 and had previously been shown to have superior cell behavior, including attachment, spreading, proliferation, and differentiation.[7b–d] A pre-osteoblast cell line, MC3T3-E1, was used as a model cell line for this study. Whereas the cells were round and less spread out on the PCL nanofiber, they were widely spread along the fibers of the PCL/fp-151 and PCL/fp-151-RGD as determined by the scanning electron microscopy (SEM) analysis of the cell morphology after one hour in the culture using a serum-free medium (the left images in Figure 3a). We also found that cell populations on PCL/MAP nanofibers increased significantly after 4 days in the culture using serum-containing media (the right images in Figure 3a). These results indicate that MAP itself provided a more favorable environment to interact with cells than did PCL. Direct cell counting was performed to quantify the degree of cell attachment and proliferation on each nanofiber. As expected, cell attachment significantly increased on the MAP-containing nanofibers compared to the PCL nanofibers, and the cells on the PCL/fp-151 nanofibers proliferated significantly more than on the PCL nanofibers after 4 days in the cell culture (Figure 3b). This proliferation was even more enhanced on the PCL/fp-151-RGD nanofiber.

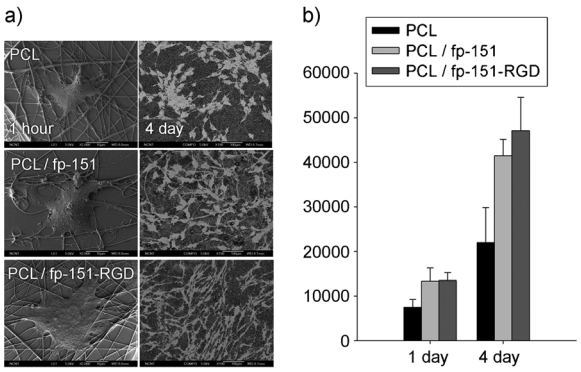

Figure 3. a) Morphology of MC3T3-E1 cells on the surface of PCL, PCL/fp-151, and PCL/fp-151-RGD nanofibers after 1 hour (left panel) and 4 days (right panel) in the culture. b) Attached cell numbers as determined by direct cell counting after 1 and 4 days in the culture.

Our results from the cell culture experiment using the PCL/MAP nanofibers, which showed good cell–nanofiber interactions and superior cell attachment and proliferation abilities, can be explained by the peculiar properties of MAPs and the effect of the bioactive peptide fused with MAP. The charged and hydrophilic surface induced by MAPs might result in the enhancement of cell attachment because it is well known that hydrophilicity is an important factor for superior cell–nanofiber interactions.[12a] Moreover, the RGD peptide has been recognized as a molecular activator of the integrin cell surface receptor, which can induce intracellular signaling pathways related to cell spreading, proliferation, and survival.[10] Especially, the activation of the integrin receptor through interactions with the RGD peptide in the initial cell attachment step could affect subsequent cell behaviors through cell signaling molecules, such as focal adhesion kinase (FAK)[10b]. Only a few studies have been reported on the surface functionalization of electrospun nanofibers with RGD peptides. Chemically conjugated RGD peptides on nanofiber surfaces have been shown to enhance fibroblast viability and the osteoblastic differentiation of stem cells.[4c,12b] However, when using the blending method of polymers with RGD peptides for electospinning, it was difficult to observe the RGD effect on cell behavior.[12c] Thus, our electrospun nanofibers that were fabricated using MAPs fused with diverse ECM peptides (including RGD[7c]) provide advantages because they do not require pretreatment and efficient exposure of the bioactive peptides are possible for the target-specific fabrication of artificial ECMs.

The biofunctionalization of the nanofibers can be also achieved by using surface coatings of various biomolecules, such as carbohydrates, proteins, and DNA. Peculiar adhesive properties of the MAP-based nanofibers could be used to immobilize various compounds, and may thus enable us to change the surface composition of nanofibers to target

specific coating molecules. To investigate the coating abilities of PCL/fp-151 nanofibers, various biomolecules, including protein, DNA, and carbohydrates, were selected as target coating molecules, and simple dipping experiments were performed. PCL, a negative control, and PCL/fp-151 = 70:30 nanofibers were immersed in each aqueous solution, including dissolved green fluorescent protein (GFP), plasmid DNA, fluorescein isothiocyanate (FITC)-conjugated hyaluronic acid (HA-FITC), and alkaline phosphatase (ALP). The results indicate that all biomolecules were uniformly coated onto the PCL/fp-151 nanofiber surface and remained uniformly coated even after intensive washings (Figure 4; lower panels), whereas there was only a little nonspecific adsorption occurred on the PCL nanofiber surface (Figure 4; upper panels). Through visualization of the ionizable moiety of

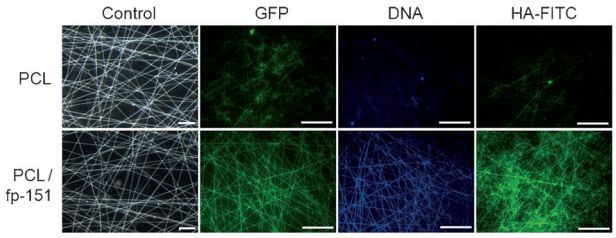

Figure 4. Fluorescence images of GFP, DNA, and HA-coated PCL and PCL/MAP nanofibers. The scale bar is 100 μm.

acidic carbohydrates using alcian blue staining,[13] we found that other acidic carbohydrates such as ECM carbohydrates, including heparan sulfate (HS) and chondroitin sulfate (CS), and brown algae-derived carbohydrate polymer, including alginic acid (AG), were all efficiently coated onto the PCL/fp-151 nanofiber surface (see Figure S6 in the Supporting Information). Furthermore, the activity of ALP, as a model enzyme, was successfully detected on the surface of the PCL/fp-151 nanofiber (see Figure S7 in the Supporting Information), thus indicating efficient immobilization of an enzyme on the nanofiber surface. In addition to the adhesive properties of MAPs, their highly positively charged surface could explain the strong binding of PCL/fp-151 nanofibers to negatively charged molecules, such as DNA and acidic carbohydrates through electrostatic interactions.

In summary, we fabricated novel, functional nanofibrous scaffolds based on MAPs, which provided a mechanically durable structural backbone with the functionality of bioactive peptides. In addition, facile functionalization of the nanofiber surfaces with various biomolecules was achieved by using the adhesive and charged properties of MAPs, without surface modifications. This novel biofunctionalized nanofiber platform that is based on MAPs could be a promising tool for successful tissue engineering applications.

Received: August 16, 2011
Revised: September 19, 2011
Published online: October 20, 2011

Keywords: biomolecules · mechanical properties · nanostructures · proteins · surface analysis

[1] C. P. Barnes, S. A. Sell, E. D. Boland, D. G. Simpson, G. L. Bowlin, *Adv. Drug Delivery Rev.* **2007**, *59*, 1413.
[2] a) D. Liang, B. S. Hsiao, B. Chu, *Adv. Drug Delivery Rev.* **2007**, *59*, 1392; b) B. M. Baker, A. M. Handorf, L. C. Ionescu, W. J. Li, R. L. Mauck, *Expert Rev. Med. Devices* **2009**, *6*, 515; c) D. R. Nisbet, J. S. Forsythe, W. Shen, D. I. Finkelstein, M. K. Horne, *J. Biomater. Appl.* **2009**, *24*, 7.
[3] a) J. Stitzel, J. Liu, S. J. Lee, M. Komura, J. Berry, S. Soker, G. Lim, M. Van Dyke, R. Czerw, J. J. Yoo, A. Atala, *Biomaterials* **2006**, *27*, 1088; b) W. He, Z. Ma, T. Yong, W. E. Teo, S. Ramakrishna, *Biomaterials* **2005**, *26*, 7606; c) M. Ziabari, V. Mottaghitalab, A. K. Haghi, *Korean J. Chem. Eng.* **2010**, *27*, 340.
[4] a) H. S. Koh, T. Yong, C. K. Chan, S. Ramakrishna, *Biomaterials* **2008**, *29*, 3574; b) Z. Ma, M. Kotaki, T. Yong, W. He, S. Ramakrishna, *Biomaterials* **2005**, *26*, 2527; c) J. R. Paletta, S. Bockelmann, A. Walz, C. Theisen, J. H. Wendorff, A. Greiner, S. Fuchs-Winkelmann, M. D. Schofer, *J. Mater. Sci. Mater. Med.* **2010**, *21*, 1363; d) J. S. Choi, K. W. Leong, H. S. Yoo, *Biomaterials* **2008**, *29*, 587.
[5] H. S. Yoo, T. G. Kim, T. G. Park, *Adv. Drug Delivery Rev.* **2009**, *61*, 1033.
[6] a) H. J. Cha, D. S. Hwang, S. Lim, *Biotechnol. J.* **2008**, *3*, 631; b) J. H. Waite, M. L. Tanzer, *Biochem. Biophys. Res. Commun.* **1980**, *96*, 1554; c) R. L. Strausberg, R. P. Link, *Trends Biotechnol.* **1990**, *8*, 53; d) H. G. Silverman, F. F. Roberto, *Mar. Biotechnol.* **2007**, *9*, 661.
[7] a) D. S. Hwang, Y. Gim, H. J. Yoo, H. J. Cha, *Biomaterials* **2007**, *28*, 3560; b) D. S. Hwang, S. B. Sim, H. J. Cha, *Biomaterials* **2007**, *28*, 4039; c) B. H. Choi, Y. S. Choi, D. G. Kang, B. J. Kim, Y. H. Song, H. J. Cha, *Biomaterials* **2010**, *31*, 8980; d) B. J. Kim, Y. S. Choi, B. H. Choi, S. Lim, Y. H. Song, H. J. Cha, *J. Biomed. Mater. Res. Part A* **2010**, *94*, 886.
[8] a) E. J. Chong, T. T. Phan, I. J. Lim, Y. Z. Zhang, B. H. Bay, S. Ramakrishna, C. T. Lim, *Acta Biomater.* **2007**, *3*, 321; b) Y. Z. Zhang, J. Venugopal, Z. M. Huang, C. T. Lim, S. Ramakrishna, *Biomacromolecules* **2005**, *6*, 2583; c) E. Schnell, K. Klinkhammer, S. Balzer, G. Brook, D. Klee, P. Dalton, J. Mey, *Biomaterials* **2007**, *28*, 3012.
[9] L. Ghasemi-Mobarakeh, M. P. Prabhakaran, M. Morshed, M. H. Nasr-Esfahani, S. Ramakrishna, *Biomaterials* **2008**, *29*, 4532.
[10] a) E. Ruoslahti, *Annu. Rev. Cell Dev. Biol.* **1996**, *12*, 697; b) F. G. Giancotti, E. Ruoslahti, *Science* **1999**, *285*, 1028; c) R. O. Hynes, *Cell* **2002**, *110*, 673.
[11] a) Y. Zhang, H. Ouyang, C. T. Lim, S. Ramakrishna, Z. M. Huang, *J. Biomed. Mater. Res. Part B* **2005**, *72*, 156; b) I. K. Kwon, T. Matsuda, *Biomacromolecules* **2005**, *6*, 2096; c) J. Lee, G. Tae, Y. H. Kim, I. S. Park, S. H. Kim, *Biomaterials* **2008**, *29*, 1872.
[12] a) X. Yang, X. Chen, H. Wang, *Biomacromolecules* **2009**, *10*, 2772; b) Y. Y. Wang, L. X. Lu, Z. Q. Feng, Z. D. Xiao, N. P. Huang, *Biomed. Mater.* **2010**, *5*, 054112; c) M. D. Schofer, U. Boudriot, S. Bockelmann, A. Walz, J. H. Wendorff, A. Greiner, J. R. Paletta, S. Fuchs-Winkelmann, *J. Mater. Sci. Mater. Med.* **2009**, *20*, 1535.
[13] S. Yamabayashi, *Histochem. J.* **1987**, *19*, 565.

